Numerical simulation of the wake of marine current turbines with a particle method

Maganga Fabrice[1], Pinon Grégory[2], Germain Grégory[1] & Rivoalen Elie[2]

April 29, 2008

[1] Hydrodynamic & Metocean, IFREMER Boulogne-sur-Mer, France,
fabrice.maganga@ifremer.fr, gregory.germain@ifremer.fr

[2] LOMC, FRE CNRS 3102, Université du Havre, France,
gregory.pinon@univ-lehavre.fr, elie.rivoalen@univ-lehavre.fr

Abstract

This paper presents numerical results for the wake behind a three bladed horizontal axis turbine in a uniform free upstream current. A three-dimensional software, initially issuing from Pinon *et al.* [6], taking into account the non stationary evolution of the wake emitted by turbine blades is developed in order to assess the disturbances generated on the sea-bed and on the free surface. So an unsteady Lagrangian method is considered for these simulations using Vortex Method. The vortex flow is discretised with particles carrying vorticity, which are advected in a Lagrangian frame.

Keywords : Vortex Method, Marine Current Turbine, Hydrodynamic.

1 Introduction

The future deployment of marine current energy converters raise questions about their impact on the environment. Modifications of the overall flow patterns in the area of current energy devices may alter the erosion and sediment transport by their wakes effects, and even the free surface of the sea. There is a concern that even a small change of these processes can cause significant impacts.

A three-dimensional software, initially issuing from Pinon *et al.* [6], taking into account for the non stationary evolution of the wake emitted by a turbine is developed in order to assess the disturbances generated on the sea-bed and on the free surface. In the present paper, we will present the numerical method and give results for wake characterisation behind a marine current turbine. The dynamics of farms consisting on numerous devices placed in close space will be analyzed in a near future.

2 Numerical methods

The first attempt of vortex method simulation was carried out by Rosenhead [8] back in 1931. To simulate an unsteady flow in an unbounded space, Rosenhead discretised the flow field with vortex blobs issuing from the edge of thin flat plate. In our case, we consider the vortex flow with particles, which are emitted at the trailing edge of the turbine blades. So an unsteady Lagrangian method is considered for these simulations using Vortex Method. The vortex flow is discretised with particles carrying vorticity, which are advected in a Lagrangian frame. The particles are emitted at the trailing edge of the turbine blades thanks to a panel method with doublet using the Kutta-Joukovski condition, as an emission scheme.

2.1 Governing equations

The flow of an incompressible fluid is governed by the Navier-Stockes equations, which are writ-

ten in velocity-vorticity formulation $(\mathbf{U}, \boldsymbol{\omega})$:

$$\frac{D\boldsymbol{\omega}}{Dt} = (\boldsymbol{\omega}.\boldsymbol{\nabla})\mathbf{U} + \nu\Delta\boldsymbol{\omega} \qquad (1)$$

$$\boldsymbol{\nabla}.\mathbf{U} = 0 \qquad (2)$$

where $\boldsymbol{\omega} = \boldsymbol{\nabla} \wedge \mathbf{U}$ is the vorticity field of the flow, $\mathbf{U}$ is the velocity field and D/Dt is the material derivative. Equation (2) is the transport equation of vortex, which is the starting point for the vortex method. $D\boldsymbol{\omega}/Dt$ represents the transport term in a lagrangian frame, $(\boldsymbol{\omega}.\boldsymbol{\nabla})\mathbf{U}$ stands for the stretching term, which disappears in two dimensions and $\nu\Delta\boldsymbol{\omega}$ accounts for diffusion. The Helmholtz decomposition of velocity field, gives :

$$\mathbf{U} = \boldsymbol{\nabla} \wedge \boldsymbol{\psi} + \boldsymbol{\nabla}\phi \qquad (3)$$

where $\boldsymbol{\psi}$ is a potential vector and ϕ is a potential. With equations (2) and (3), we obtain :

$$\Delta\phi = 0 \quad \text{and} \quad \Delta\boldsymbol{\psi} = -\boldsymbol{\omega} \qquad (4)$$

The rotational component of the velocity field $\mathbf{U}_\omega$ is connected to the vorticity field by the Biot-Savart law, equation (5) :

$$\mathbf{U}_\omega(\mathbf{r}) = \frac{1}{4\pi}\int_v \mathbf{K}(\mathbf{r} - \mathbf{r}') \wedge \boldsymbol{\omega}(\mathbf{r}')dv' \qquad (5)$$

with $\mathbf{K}(\mathbf{r}) = \frac{\mathbf{r}}{\mathbf{r}^3}$. In order to avoid collapse of the computations when two particles are going close together, a desingularised kernel $\mathbf{K}_\delta(\mathbf{r})$ is used (equation (6)) as in Lindsay & Krasny [5].

$$\mathbf{K}_\delta(\mathbf{r}) = \frac{\mathbf{r}}{(\mathbf{r}^2 + \delta^2)^{3/2}} \qquad (6)$$

This desingularised kernel is commonly used in the lagrangian vortex community; several references can be consulted on that particular topic, amongst other the book of Cottet & Koumoutsakos [3]. On top of that, we developed the *Tree Code* alogorithm developed by Lindsay & Krasny [5], based on a Taylor expansion on the kernel $\mathbf{K}_\delta(\mathbf{r})$ in order to speed up the determination of the velocity $\mathbf{U}_\omega(\mathbf{r})$ in equation (5).

The potential velocity $(\mathbf{U}_\phi = \boldsymbol{\nabla}\phi)$ will be defined in order to account for the turbine blades. The turbine blade surface (S) is discretised into N_p surface elements, each surface element has a normal unit vector $\mathbf{n}$ and a surface ds. P is a control point located at the center of the considered surface element of the turbine blade. A slip condition (equation (7)) is imposed at every control point P of the considered surface element and the potential velocity inducted by

these boundary elements must satisfy conditions (7) and (8) :

$$\frac{\partial\phi}{\partial\mathbf{n}} = -\mathbf{U}.\mathbf{n} \qquad (7)$$

$$\lim_{\mathbf{r}\to\infty} \boldsymbol{\nabla}\phi = 0 \qquad (8)$$

This last potential velocity is calculated thanks to equations (7) and (8) and the third Green's relation :

$$\phi(M) = \frac{1}{4\pi}\iint_S \mu(P)\frac{\mathbf{MP}.\mathbf{n}(P)}{|\mathbf{MP}|^3}ds, \qquad (9)$$

M being any point of the flow field, $\mu(P)$ representing a distribution of normal doublet on the turbine blade surface (S). Assuming that the doublet contribution $\mu(P)$ is constant on the surface element and equal to μ_P, the velocity component $\mathbf{U}_\phi$ is defined as :

$$\mathbf{U}_\phi = \frac{1}{4\pi}\sum_{p=1}^{N_p} \mu_P\boldsymbol{\nabla}_M\frac{\mathbf{MP}.\mathbf{n}(P)}{|\mathbf{MP}|^3}ds_p \qquad (10)$$

In order to determine the normal doublet repartition μ_P on the blade surface (S), we define a matrix system (equation (11)) using a slip condition equation (7). This slip condition is written in the form of a linear system :

$$[\mathbf{A}][\boldsymbol{\mu}] = [\mathbf{U}_{SM}] \qquad (11)$$

and the generation flow can be included in a matrix where :

- $[\mathbf{A}]$ is the influence matrix, obtained thanks to equation (10), representing the turbine blades presence,

- $[\boldsymbol{\mu}]$ is an unknown vector representing the doublet distributions,

- $\mathbf{U}_{SM}$ is the second member, to enforce the slip condition (7), representing the velocity on the blade control point P owing the presence of the particles $\mathbf{U}_\omega$, the main stream velocity $\mathbf{U}_\infty$ and the blade rotation velocity.

The influence matrix only depends on the grid of the blade and can therefore be reversed.

2.2 Discretisation

The first step consists in discretising the vorticity field into vortex elements, which are termed either blobs or particles indifferently hereafter. Then in a second step, these particles are advected thanks to the velocity field. In order to define the position of the particles, dv is assumed to be a small volume whose support is P_i. The

$\mathbf{X}_i$ position of the ith particle and the vorticity $\mathbf{\Omega}_i$ carried by this particle are respectively defined by :

$$\mathbf{X}_i = \frac{\int_{P_i} x dv}{\int_{P_i} dv} \quad \text{and} \quad \mathbf{\Omega}_i = \int_{P_i} \boldsymbol{\omega} dv \qquad (12)$$

The Kutta-Joukovski condition is used to obtain the vorticity, that has to be introduced in the emitted vortex blobs. The position $\mathbf{X}_i$ and the weight $\mathbf{\Omega}_i$ of the emitted particle from the jth linear element discetising the trailing edge is obtained as follows :

$$\begin{aligned}
\mathbf{X}_i &= \mathbf{X}_j + \mathbf{U}_j(\frac{\delta t}{2}) \\
\mathbf{\Omega}_i &= |\mathbf{U}_j|\delta t \int_{\delta h_j} \overline{\boldsymbol{\omega}} dh
\end{aligned}$$

where $\mathbf{U}_j = (\mathbf{U}_{inside} + \mathbf{U}_{outside})/2$ is the mean velocity onto the considered element between the inside and the outside of the turbine blade, δh_j is the width of the discrete element and $\overline{\boldsymbol{\omega}} = \mathbf{n} \wedge (\mathbf{U}_{inside} - \mathbf{U}_{outside})$. On top of that, we added a particles' emissions scheme for the blade tip in a similar way as described above.

The evolution equation of vortex depends on the position of particles $\mathbf{X}_i$ and on the quantity of transported vorticity $\mathbf{\Omega}_i$:

$$\frac{D\mathbf{X}_i}{Dt} = \mathbf{U}_i \qquad (13)$$

$$\frac{D\mathbf{\Omega}_i}{Dt} = (\mathbf{\Omega}_i.\boldsymbol{\nabla})\mathbf{U}_i + \nu\Delta\mathbf{\Omega}_i \qquad (14)$$

$\mathbf{U}_i = \mathbf{U}(\mathbf{X}_i)$ and $\mathbf{U}$ is the sum of all the velocity contributions defined as :

$$\mathbf{U} = \mathbf{U}_\infty + \mathbf{U}_\phi + \mathbf{U}_\omega \qquad (15)$$

with

$\mathbf{U}_\infty$: infinite velocity field upstream the flow,

$\mathbf{U}_\omega$: velocity field induced by the vortex which is calculated in equation (5),

$\mathbf{U}_\phi = \boldsymbol{\nabla}\phi$: potential velocity field.

The diffusion term is discretised with the PSE (Particle Strength Exchange) method [2, 4], which has a straigth-forward three-dimensional version. However, for the present paper, only inviscid computations will be presented.

To avoid collapse of the calculation, a global remeshing of the particles was also included every four time steps in these simulations. This remeshing uses the interpolation formula M_4'. A more complete survey of the effect of global remeshing is available in a following references [3], where different interpolation formulas have been studied in terms of the L_2 velocity error introduced in the simulation. These studies concluded that the third order interpolation formula M_4' provides a good compromise between accuracy, smoothness of the results and implementation's work. Amongst the numerical aspects treated in this section is also the integration scheme. A second order Runge-Kutta is used as the time integration scheme for these simulations in order to have a good compromise between accuracy and time saving. Those simulations are run on parallel architectures thanks to the MPI (Message Passing Interface) libraries.
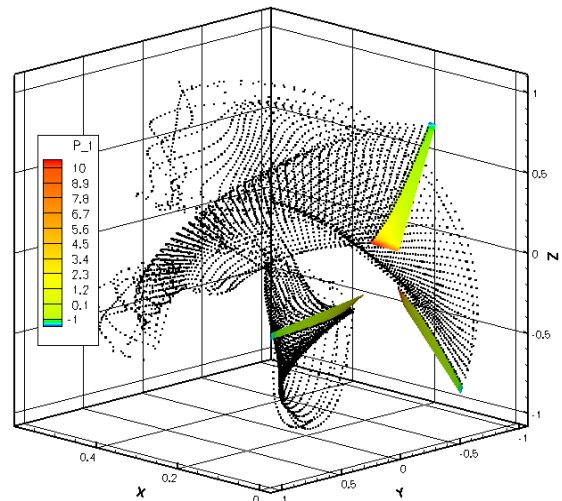
3 First results

Figure 1: *Visualisation of non dimensional total pressure on the blades and emitted particles in the near wake region, early development of the wake (50th iteration) without remeshing.*

In order to test the method, we run different simulations on a three bladed horizontal axis turbine in a uniform upstream current. The shape of the blades is defined similarly to those of Bahaj *et al.* [1] (initial description with additional 5 degree pitch), with the same blade radius R equal to $0.4\,m$. The free stream velocity U_∞ has been set similarly to $1.4\,m/s$ and we imposed a rotational speed Ω in order to have a tip speed ratio $TSR = \frac{\Omega R}{U_\infty} = 5.0$. We run the computation dimensionless so that all the result will be presented non dimensional. This corresponds to the early development of the wake. The blades are discretised into $N_p = 360$ mesh elements with 40 particles emitted at each blade's trail-

3

ing edge for each time step $dt = 0.015 \, s$. As presented earlier, the presented computation was run inviscid, on a cluster of 8 processors (Intel Xeon Quad Core duo, 2.66GHz) for approximately 2 hours in order to have the first 200th unsteady time steps.

On figure 1, one can observe the total pressure distribution on the blades and the emitted particles in the wake for an early stage of the unsteady simulation (50th iteration). Each blade's wake can be clearly identified owing to the fact that no remeshing has been proceeded on the computation yet. The determination of the pressure has been realised thanks to a technics presented in Rouffi [7].

$$C_P = \frac{Q \Omega R}{0.5 \rho \pi R^2 U_\infty^3} \qquad (16)$$

$$C_T = \frac{T}{0.5 \rho \pi R^2 U_\infty^2} \qquad (17)$$

Work still need to be done in order to have a complete validation of the method. Concerning *Power Coefficent* C_P (equation 16), with Q the rotational speed torque, and *Thrust Coefficent* C_T (equation 17), with T the thrust. For the moment, we have a relatively good agreement with respect to the numerical and experimental results of Bahaj *et al.* [1]. However, a possible remaining source of error stands in the fact that we did not take into account for the turbine rotor hub itself. Additional tests are currently realised on that topic (*i.e* $C_P = f(TSR)$) in order to have a good confidence in the method. We already know that for large TSR, results will not fit to the experiments as we do not have any account for the boundary layer detachment on the blade.
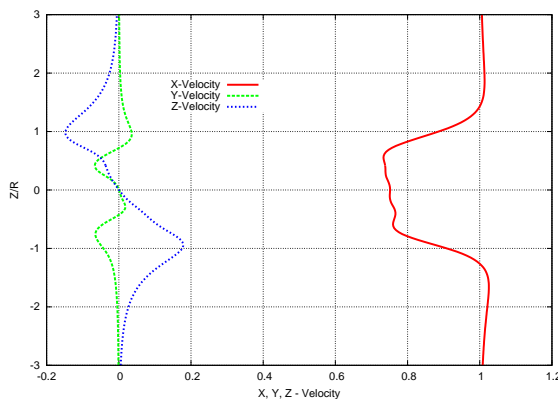

Figure 2: *X, Y, Z-mean velocity profile located in the near wake of the turbine at $x/R = 1.0$ in the central section.*

Concerning the velocity characteristics in the wake, figure 2 presents some velocity profiles in the central section of the wake for the dimensionless coordinate $x/R = 1.0$. The mean velocity profiles has been obtained by averaging 11 unsteady configurations (every 10 iterations) between the 100th and the 200th iterations. The lack of symetry in the results, especially the X-velocity profile (see figures 2 and 3), stands in the fact that the average has not been realised on a sufficiently large panel of unsteady instantaneous configurations. As soon as the simulation will be proceeded on larger time (*i.e* ≈ 1000 unsteady time steps), the quality of the result will be enhanced. Vertical velocity profile (U_z) shows a contraction of the wake, which is completely coherent with the former experimental observations.
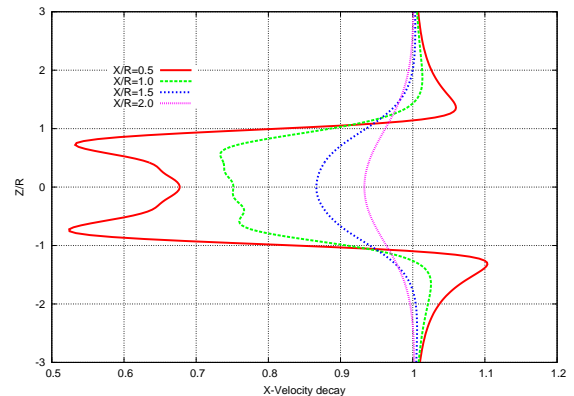

Figure 3: *X-mean velocity profile for different locations in the wake of the turbine in the central section.*

Concerning the X-velocity deficit in the wake, figure 3 presents some X-velocity profiles for different locations in the wake of the turbine. One can see that the longitudinal velocity profiles (U_x) show a maximum velocity deficit in the wake, which is close to 50% of the upstream velocity. This appears to be an underestimating result, probably due to the same reason as above, that is to say the absence of rotor hub in the centre of the whole turbine. This supposition is clearly validated as soon as we look at the $X/R = 0.5$ profile for instance. On this profile, we can observe that the maximum velocity deficit is not located at the centre of the turbine ($Y = 0.0$ and $Z = 0.0$). In fact, as the rotor hub is not considered yet, the flow can go through the centre of the turbine, which locally acts as a *Venturi*. This problem will be adressed in the closing remarks paragraph. On this particular profile, we can also observe an acceleration of

the flow at the top end of the blade. This acceleration can be explained by the blockade effect of the whole turbine. The last observation concern the velocity deficit decay as X/R increases. We can observe that the velocity profile returns to the main stream velocity very quickly, probably more rapidly as it should. This observation cannot be clearly quantified yet because, to our knowledge, there is no data available for this turbine in the litterature in order to compare with our results. From these observations, we can make two remarks :

- Experiments will be soon carried out in the free surface circulation flume tank of Ifremer. With these experimental results, we will be able to compare more qualitatively and quantitatively this numerical work,

- With the account of the whole structure in the simulation, blades and rotor hub, together with computations realised on a larger time, we will probably improve the quality of the results.
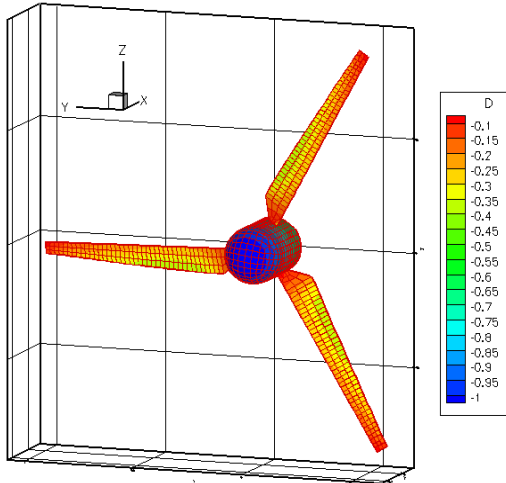
4   Closing remarks and perspectives

Figure 4: *Instantaneous surface normal doublet repartition on a 3-bladed horizontal axis turbine with rotor hub, discretised into* 780 *elements.*

Figure 4 shows a 3-bladed horizontal axis turbine, discretised into 780 elements, where the rotor hub is considered entirely. For the moment, preliminary computations show that the results are improving but the computation durations are increasing with the number of mesh elements. This increase is actually due to the fact that the inversion of the matrix system (equation (11)) is not optimised and is also sequential, which is time consumming. Numerical improvements are now under realisation. At the same time, some experiments will be carried out in the free surface circulation flume tank of Ifremer Boulogne-sur-Mer. They will be used to validate this numerical work. Other aspects are going to be introduced in the computation, for instance a velocity gradient in order to account for the boundary layer at the sea-bed, an unsteady velocity fluctuation due to the influence of the heave on the main current, and finally the influence of the free surface close to the turbine. Similar configurations tests are possible in the Ifremer flume tank. With these experiments, we will be able to analyse the effects of the wake emitted by this type of structure starting from the characteristics of the flow to the periphery of the system.
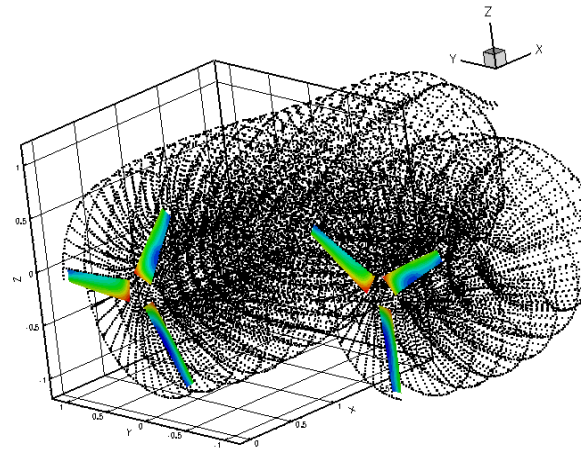

Figure 5: *Schematic explaination of possible turbine-wake interaction, which will be computated in the near future.*

The development of this numerical code is still in progress. The free surface, boundary layer velocity profile and an unsteady fluctuation of this profile will be implemented step by step in order to take into account for the global environment of marine current turbines. The first results given here will be extended in the near future. These numerical tools could be used prior to the installation of a marine current turbine farm, with the aim to examine and assess its potential environmental impact. Understanding the effect these devices have on the flow is also critical in determining how one device may mod-

ify both the performance of and loading experienced by another device in an array, as the schematic picture of figure 5 explains.

References

[1] A.S. Bahaj, W.M.J Batten and G. Mc-Cann. Experimental verifications of numerical predictions for hydrodynamic performance of horizontal axis marine current turbines. Renewable Energy, 32 : 2479-2490, 2007.

[2] J.P. Choquin and S.Huberson. Particles simulation of viscous flow. Computers & Fluid, 17(2): 397-410, 1989.

[3] G.H. Cottet and P.D. Koumoutsakos. Vortex method: Theory and practice. Cambridge University Press, UK, 2000.

[4] P. Degond and S. Mas-Gallic. The weighted particle method for convection-diffusion equations. Math. Comput., 53: 485-508, 1989.

[5] K. Lindsay and R. Krasny. A particle method and adaptive treecode for vortex sheet motion in three-dimensional flow. J. Comput. Phys. Vol 172, 2001.

[6] G. Pinon, H. Bratec, S. Huberson, G. Pignot and E. Rivoalen. Vortex method for the simulation of a 3D round jet in a cross-stream. J. Turbulence, Vol. 6 N18, 2005.

[7] F. Rouffi. Résolution numérique de problèmes non linéaires de l'hydrodynamique navale : manœuvrabilité et tenue à la mer des navires. PhD thesis, Université Pierre et Marie Curie, 1992.

[8] L. Rosenhead. The formation of vortices from a surface of discontinuity. Proc. Soc. London, A(134): 170-192, 1931.